Density Profile and Fluctuation Measurements by Microwave Reflectometry on EAST

2014 Plasma Sci. Technol. 16 311

(http://iopscience.iop.org/1009-0630/16/4/02)

Density Profile and Fluctuation Measurements by Microwave Reflectometry on EAST*

ZHANG Shoubiao (张寿彪), GAO Xiang (高翔), LING Bili (凌必利),
WANG Yumin (王嵎民), ZHANG Tao (张涛), HAN Xiang (韩翔),
LIU Zixi (刘子奚), BU Jingliang (布景亮), LI Jiangang (李建刚) and EAST team

Institute of Plasma Physics, Chinese Academy of Sciences, Hefei 230031, China

Abstract A microwave reflectometry system operating in the V-band frequency with extraordinary mode polarization has been developed on the EAST tokamak. The reflectometry system, using a voltage-controlled oscillator (VCO) source driven by an arbitrary waveform generator with high temporal resolution, can operate for the density profile measurement. The result of the bench test shows that the output frequency of the VCO has a linear dependence on time. The dispersion of reflectometry system is determined and reported in this paper. The evolution of a pedestal density profile during the L-H transition is observed by the reflectometry in H-mode discharges on EAST tokamak. A frequency synthesizer is used to replace the VCO as microwave source for density fluctuation measurements. The level of density fluctuation in the pedestal shows an abrupt decrease when the plasma enters into H-mode. A coherent mode with a frequency of about 100 kHz is observed and the mode frequency decreases gradually as the pedestal evolves.

Keywords: microwave reflectometry, pedestal, density fluctuation, EAST

PACS: *52.70.Gw*

DOI: 10.1088/1009-0630/16/4/02

(Some figures may appear in colour only in the online journal)

1 Introduction

Microwave reflectometry is a radar-like technique, which measures the phase or time delay of electromagnetic radiation reflected from a plasma cutoff layer. The diagnostic is widely used on tokamak and other fusion devices [1−5]. Reflectometry has the great advantage of being a non-perturbative method of measurement due to very low injected power of the probing microwave beam. Reflectometry has been developed for two main applications: determination of density profile and density fluctuations. Due to its high temporal and spatial resolution, reflectometry for density profile measurement becomes an important tool to do physics studies, such as H-mode physics, transport behavior, etc. For the measurement of density profile, it is well known that density fluctuations may seriously deteriorate the accuracy of density measurement, and the ultrafast sweep reflectometry [6,7] can overcome this deterioration by "freezing" the fluctuations. Reflectometry is also a powerful tool to determine some characteristics of the density fluctuations, which could induce phase fluctuation of the microwave signal [1].

The high confinement mode (H-mode) was first discovered in the ASDEX tokamak [8]. Since then, lots of work has been done to understand the H-mode physics with significant progress achieved in experiments and theories. The H-mode is characterized by a spontaneous formation of a transport barrier at the plasma edge, which is usually associated with the repetitive edge localized modes (ELMs). The measurement of the dynamic evolution of density profile is important for understanding the L-H transition, pedestal and ELM physics. Recently, H-mode has been achieved on the experimental advanced superconducting tokamak (EAST) [9,10]. EAST is a full superconducting toroidal device with a major radius (R) of 1.75 m and a minor radius (a) of 0.45 m. An X-mode microwave reflectometry with probing frequency 46-74 GHz has been developed on EAST, which can provide routine measurement of the edge density profiles and fluctuations. In this paper, the reflectometry setup and some experimental results are presented.

This article is organized as follows: the development of reflectometry on EAST is described in section 2, and the experimental results are given in section 3. Summary and future plans are presented in section 4.

2 Development of reflectometry

2.1 Description of the reflectometry system

A schematic of the X-mode reflectometry system on EAST is shown in Fig. 1. The microwave source

*supported by National Natural Science Foundation of China (Nos. 11305208 and 11275234) and the National Magnetic Confinement Fusion Program of China (Nos. 2014GB106000 and 2014GB106003)

of the reflectometry is a voltage-controlled oscillator (VCO), which generates frequencies between 11.5 GHz and 18.5 GHz with output power ranging from 21 dBm to 24 dBm. The output wave of the VCO, driven by an arbitrary waveform generator (AWG), is split into two channels using a 3 dB power divider. One channel is used as a reference arm and the other is used as a probing arm. To achieve heterodyne detection, the probing wave frequency is modulated in a single sideband modulator (SSBM) by a quartz oscillator at 100 MHz. The frequency of output wave from the SSBM is upshifted 100 MHz and then upconverted by an active quadrupler, providing frequency coverage between 46 GHz and 74 GHz with an output power ranging from 8 dBm to 12 dBm. Two adjacent antennae, located at the equatorial plane of the low field side of EAST, are used for emission and reception. A 3 m delay line is used to compensate for the phase delay of the reference channel. After the quadrupling of its frequency, the reference wave is mixed with the reflected wave from the plasma. The I/Q detector is used to measure the in-phase and 90°-phase signals which allow the absolute phase and amplitude detection. For the measurements of density fluctuations, the VCO source is replaced by a frequency synthesizer, which has lower noise and smaller drift.

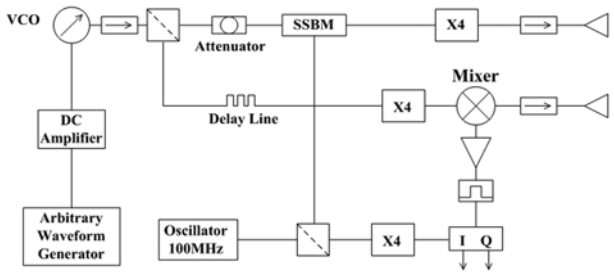

Fig.1 Schematic diagram of the V-band X-mode reflectometry on EAST

The condition for the absorption and reflection of waves in a magnetized plasma is governed by the refractive index, which is given by the Appleton-Hartree equation. For X-mode polarized waves, reflection occurs at the position where the probing wave frequency equals the right-hand cutoff frequency ($\omega_{\rm R}$) or left-hand cutoff frequency ($\omega_{\rm L}$), which are given by

$$\omega_{\rm R,L}^2 = \frac{1}{2}\left[(2\omega_{\rm p}^2+\omega_{\rm c}^2) \pm \omega_{\rm c}\sqrt{4\omega_{\rm p}^2+\omega_{\rm c}^2}\,\right], \qquad (1)$$

where $\omega_{\rm c} = eB/m_{\rm e}$ is the electron cyclotron frequency and $\omega_{\rm p} = \sqrt{n_{\rm e}e^2/\varepsilon_0 m_{\rm e}}$ the plasma frequency. Fig. 2 shows the characteristic plasma frequencies on the equatorial plane by assuming a parabolic density profile with central density of 3.5×10^{19} m^{-3} in typical EAST discharge with toroidal magnetic field ($B_{\rm t}$) of 1.85 T at R_0=1.88 m. Using the right-hand polarized probe waves, the present V-band system covers the plasma profile from R ~2.1 m to R ~2.3 m as seen from the figure. One of the advantages of the X-mode reflectometry is that the plasma edge location can be determined by the signal characteristics, as shown in section 3. Other advantages of X-mode as compared to O-mode propagation are the ability to look beyond the density peaks and the compatibility with flat H-mode density profiles, due to the magnetic field dependence of the refractive index.

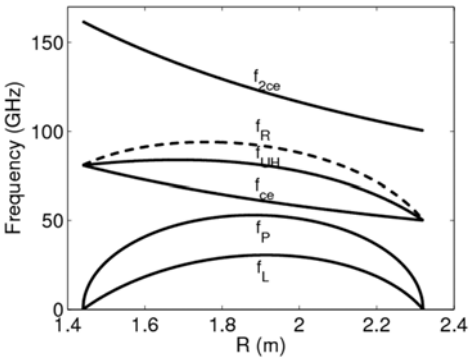

Fig.2 Characteristic frequencies on the equatorial plane for typical EAST tokamak parameters. $f_{\rm ce}$: electron cyclotron frequency, $f_{\rm p}$: plasma frequency, $f_{\rm L}$: left-hand cutoff frequency, $f_{\rm R}$: right-hand cutoff frequency, $f_{\rm UH}$: upper hybrid frequency, $f_{\rm 2ce}$: second harmonic of the electron cyclotron frequency

2.2 Bench test of reflectometry system

Fig. 3 shows the nonlinear dependence of the output wave frequency of the VCO on the driving voltage, which is measured by changing the driving voltage step by step. Considering this dependence, a nonlinear waveform of driving voltage is programmed into the AWG, and is expected to acquire a linear sweeping of the output wave frequency of the VCO. The system test in laboratory has been done to check the linearity of the sweeping frequency and determine the system dispersion.

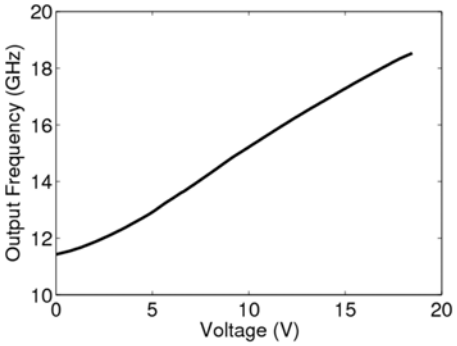

Fig.3 The dependence of static output frequency of VCO on driving voltage

By putting a metallic mirror in front of the antennas, the phase delay (ϕ) of the probing and reference channel was measured. According to the principle of reflectometry, the relationship between delay time (τ) and the phase delay is

$$\tau = \frac{1}{2\pi}\frac{{\rm d}\phi/{\rm d}t}{{\rm d}f/{\rm d}t}, \qquad (2)$$

where f is the probing frequency. In the test, delay time (τ) consists of two parts, the delay time ($\tau_{\rm v}$) due to the

wave propagation in vacuum and the delay time (τ_s) due to the wave propagation in the microwave circuit.

$$\tau = \tau_v + \tau_s = \frac{1}{2\pi}\frac{d\phi/dt}{df/dt}. \quad (3)$$

The time delay $\tau_v = 2d/c$ is related only to the distance (d) between antennae and the metallic mirror, and τ_s is dependent on f, representing the system dispersion.

The phase delay has been measured for different distances. For any two different distances d_1 and d_2, the relationship between the phase delay difference ($\Delta\phi$) and the time delay difference ($\Delta\tau_v$) is used since the τ_s doesn't depend on d.

$$\Delta\tau_v = \frac{2\Delta d}{c} = \frac{1}{2\pi}\frac{d\Delta\phi/dt}{df/dt}. \quad (4)$$

Here, $\Delta d = d_1 - d_2$. After a simple manipulation, one can get

$$f(t) = f_0 + \frac{c}{4\pi\Delta d}[\Delta\phi(t) - \Delta\phi_0], \quad (5)$$

where f_0 and $\Delta\phi_0$ are the probing wave frequency (46 GHz in the test) and phase delay difference at the initial time of one sweeping cycle, respectively. Fig. 4 shows the time dependence of the sweeping frequency calculated by using Eq. (5) for three different ΔT, where ΔT is the repetition rate between sweeps. The result shows that linearity of the sweeping frequency is very good up to a repetition rate of 50 μs.

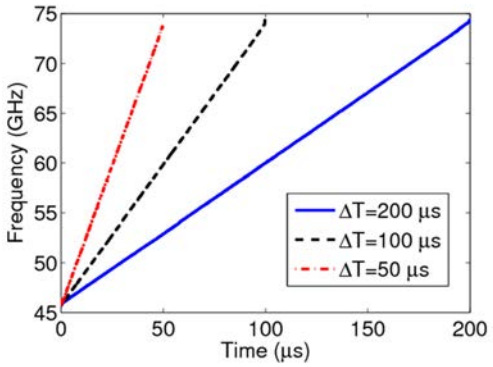

Fig.4 Output frequency of VCO after calibration with different repetition rates ΔT between sweeps

The system dispersion has been calculated from the following formula,

$$\tau_s = -\tau_v + \frac{1}{2\pi}\frac{d\phi/dt}{df/dt}. \quad (6)$$

Fig. 5 shows the dependence of τ_s on the probing frequencies. It can be observed that the dispersion is mainly in the low frequency range and doesn't depend on ΔT. In the experiment, the system dispersion is considered in the density profile reconstruction.

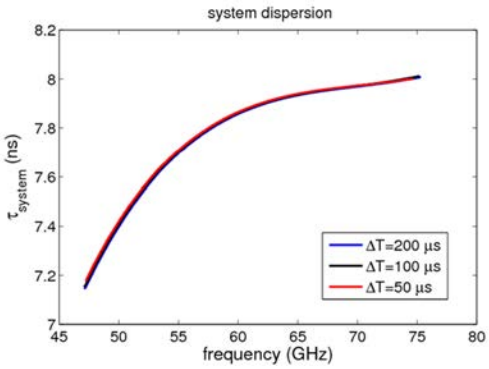

Fig.5 The dependence of reflectometry system dispersion on probing frequency

3 Experimental results

In the discharges with a high B_t of 2.25 T on EAST tokamak, edge density profile has been measured by the V-band X-mode reflectometry. Fig. 6(a) shows the line-averaged density measured by interferometry in one such high B_t plasma discharge. The line-averaged

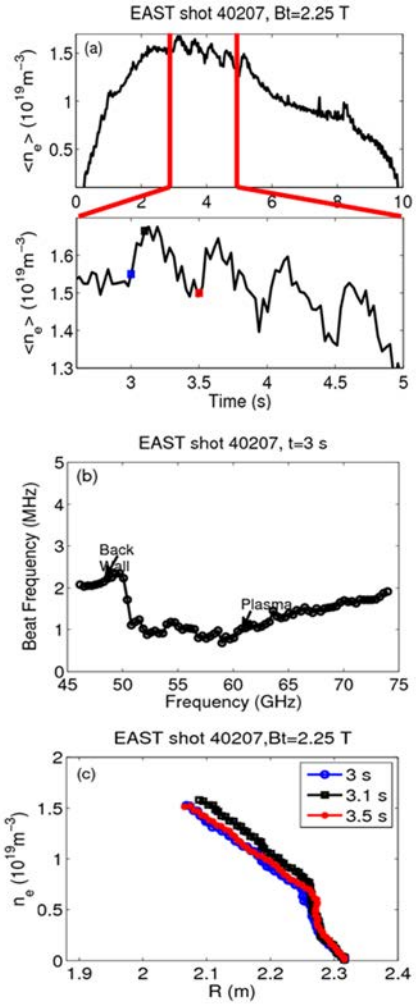

Fig.6 (a) The line-averaged density from HCN laser interferometry on EAST, (b) The dependence of beat frequency on probing frequency in one sweeping cycle, (c) Density profiles reconstructed by the reflectometry system at different time slices

density shows several peaks from 2.5 s to 5 s due to density modulation using gas puffing. Fig. 6(b) shows the beat frequency f_b in one sweeping cycle (ΔT=200 μs) at the time of 3 s. Here, f_b is equal to $\frac{d\phi/dt}{2\pi}$ in Eq. (2) and is analyzed by applying Choi-Williams distribution [11]. Below 51 GHz, the probing wave is reflected from the wall, and the beat frequency decreases quickly when the probing wave is above 51 GHz and reflected from the edge plasma. By using the information of magentic field, the density profiles were reconstructed at different time as shown in Fig. 6(c). The density from R=2.10 m to R=2.25 m at the time of 3.1 s, corresponding to one peak in line-averaged density (Fig. 6 (a)), is larger than that at the time of 3.0 s. The density profile is then recovered at 3.5 s, which is similar to that at 3.0 s. This indicates that the evolution of the density profile measured by reflectometry is consistent with that of the line-averaged density measured by interferometry.

Fig. 7(a) shows that the L-H transition in EAST shot 40786 occured at about 3.48 s when the D_α signal showed an abrupt decrease and both the line-averaged density and MHD energy began to increase. Due to the low magnetic field in H-mode discharges on EAST, usually 1.85 T like this shot, the reconstruction of density profile from the measurement of the reflectometry needs the edge profile provided by other diagnostics. Fig. 7(b) shows density profiles at different time slices

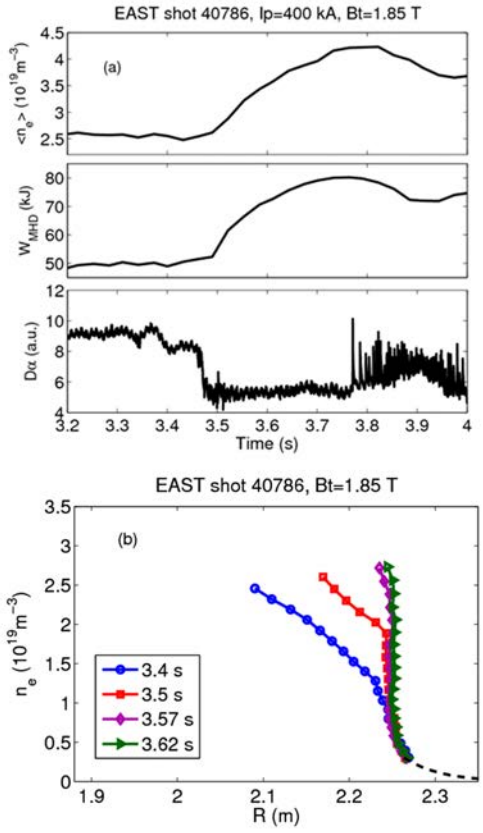

Fig.7 Plasma density profile during L-H transition from the reflectometry in shot 40786 on EAST. (a) Line-averaged density and MHD energy increase, and D_α signal decrease in L-H transition, (b) Edge density profile at different time from the reflectometry during L-H transition

in shot 40786 by using the edge profiles measured by edge Langmuir probe in another similar shot. It can be seen from this figure that the edge pedestal formed at t=3.5 s just after the L-H transiton and the density and density gradient gradually increase with time.

The density fluctuation evolution during L-H transition on EAST tokamak has been measured by reflectometry, as shown in Fig. 8. The L-H transition for shot 41713 occors at about 3.275 s at which D_α signal shows an abrupt decrease. The fluctuation reflectometry (using the frequency synthesizer as source) with the probing frequency of 54 GHz, corresponding to a cutoff at normalized radius $r \sim 0.95$, is used to measure the density fluctuation. Fig. 8(b) shows that the density fluctuation level also has an abrupt decrease at the time of L-H transition and the plasma stays in this low fluctuation stage for about 20 ms. During this low fluctuation stage, the high frequency component of density fluctuation is suppressed compared with the L-mode plasma shown in Fig. 8(c). A coherent mode with frequency of about 100 kHz is observed in the density fluctuation spectrum, and the density fluctuation level increases accordingly after the low fluctuation stage. In addition, the coherent mode frequency gradually decreases as the pedestal evolves. The coherent modes are often seen in the H-mode pedestal region of ELM-free H-modes in EAST and other tokamak devices [12,13]. The role of the coherent mode in particle and energy transport in the pedestal region is unclear at this moment.

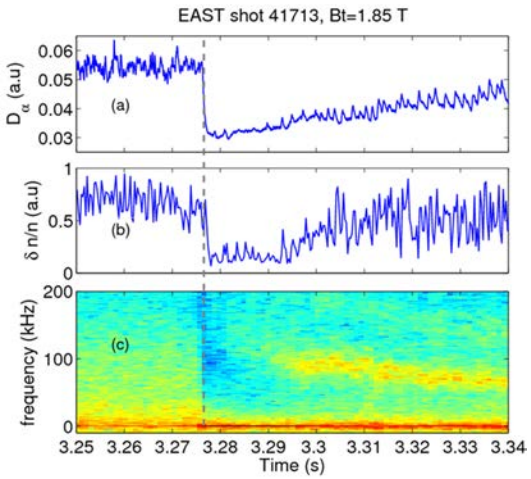

Fig.8 (a) D_α signal, (b) Density fluctuation level ($\delta n/n$), (c) Fluctuation spectrum measured by a 54 GHz reflectometry (with cutoff at about normalized radius of ~0.95) for shot 41713 on EAST

4 Summary

A 46-74 GHz X-mode reflectometry has been developed to measure the plasma density profiles and fluctuations on EAST. Through the bench test of reflectometry system, the linearity of sweeping frequency was proved and the system dispersion was determined. The density pedestal formation and evolution in the H-mode plasma have been clearly observed by the reflectometry.

During the L-H transition, a coherent mode of 100 kHz has been measured by fluctuation reflectometry with probing frequency at 54 GHz.

32-50 GHz (Q-band) and 72-110 GHz (W-band) reflectometries are under development. The combination of the three reflectometries will provide dynamic evolutions of the density profile for the physical studies of the L-H transition, pedestal and ELM physics.

Acknowledgments

The authors would like to thank Dr. Z. B. Shi, Dr. W. W. Xiao, Dr. X. L. Zou, Dr. T. Tokuzawa and Dr. A. D. Liu for their helpful discussions.

References

1 Mazzucato E. 1998, Review of Scientific Instruments, 69: 2201
2 Laviron C, Donne A J H, Manso M E, et al. 1996, Plasma Phys. Control. Fusion, 38: 905
3 Lin Y, Irby J, Stek P, et al. 1999, Review of Scientific Instruments, 70: 1078
4 Tokuzawa T, Kawahata K, Pavlichenko R O, et al. 2001, Review of Scientific Instruments, 72: 328
5 Clairet F, Sabot R, Bottereau C, et al. 2001, Review of Scientific Instruments, 72: 340
6 Wang G, Doyle E J, Peebles W A, et al. 2004, Review of Scientific Instruments, 75: 3800
7 Meneses L, Cupido L, Sirinelli A, et al. 2008, Review of Scientific Instruments, 79: 10F108
8 Wagner F. 1982, Phys. Rev. Lett., 49: 1408
9 Liu Z X, Gao X, Zhang W Y, et al. 2012, Plasma Phys. Control. Fusion, 54: 085005
10 Xu G S, Wan B N, Li J G, et al. 2011, Nucl. Fusion, 51: 072001
11 Zhong W L, Shi Z B, Zou X L, et al. 2011, Review of Scientific Instruments, 82: 103508
12 Slusher R E, Surko C M, Valley J F, et al. 1984, Physical Review Letter, 53: 667
13 Tynan G R, Schmitz L, Blush L, et al. 1994, Physics of Plasmas, 1: 3301

(Manuscript received 26 October 2012)
(Manuscript accepted 3 May 2013)
E-mail address of corresponding author GAO Xiang: xgao@ipp.ac.cn